

OPEN ACCESS

EDITED BY

Qianman Peng,

Harvard Medical School, United States

REVIEWED BY

Joachim Neumann,

Institut für Pharmakologie und Toxikologie,

Germany

Marko Ravic,

University of Kragujevac, Serbia

Mingjie Zheng,

University of Texas Health Science Center at

Houston, United States

Ke Song,

Sichuan University, China

*CORRESPONDENCE

Wu Xiaolin,

⊠ wxling.23@163.com

Zhao Yugin,

⊠ zyq7310@qq.com

¹These authors have contributed equally to this work

RECEIVED 22 April 2025 ACCEPTED 08 September 2025 PUBLISHED 31 October 2025

CITATION

Qi R, Jingjing Z, Hongchang G, Chenyu L, He H, Juan L, Yuqin Z and Xiaolin W (2025) Agonizing GABA_BR suppresses GLP-1RA's chronotropic effect and reduces post-myocardial infarction arrhythmogenesis. Front. Pharmacol. 16:1616181. doi: 10.3389/fphar.2025.1616181

COPYRIGHT

© 2025 Qi, Jingjing, Hongchang, Chenyu, He, Juan, Yuqin and Xiaolin. This is an open-access article distributed under the terms of the Creative Commons Attribution License (CC BY). The use, distribution or reproduction in other forums is permitted, provided the original author(s) and the copyright owner(s) are credited and that the original publication in this journal is cited, in accordance with accepted academic practice. No use, distribution or reproduction is permitted which does not comply with these terms.

Agonizing GABA_BR suppresses GLP-1RA's chronotropic effect and reduces post-myocardial infarction arrhythmogenesis

Run Qi^{1,2,3†}, Zhang Jingjing^{4,5,6†}, Gu Hongchang^{1,2†}, Li Chenyu³, Hu He^{1,2}, Li Juan^{1,2}, Zhao Yuqin^{1,2*} and Wu Xiaolin^{1,2,3*}

¹Department of Cardiology, Xiangyang Central Hospital, Affiliated Hospital of Hubei University of Arts and Science, Xiangyang, Hubei, China, ²Institute of Cardiovascular Diseases, Xiangyang Central Hospital, Affiliated Hospital of Hubei University of Arts and Science, Xiangyang, Hubei, China, ³Hubei Key Laboratory of Biological Targeted Therapy. Union Hospital, Tongji Medical Collage, Huazhong University of Science and Technology, Wuhan, Hubei, China, ⁴Department of Cardiology, Renmin Hospital of Wuhan University, Wuhan, Hubei, China, ⁵Department of Electrophysiology, Cardiovascular Research Institute of Wuhan University, Wuhan, Hubei, China, ⁶Department of Electrophysiology, Hubei Key Laboratory of Cardiology, Wuhan, Hubei, China

Background: Glucagon-like peptide-1 receptor agonists (GLP-1RAs) have been reported to improve cardiovascular outcomes, potentially through glucose metabolism-independent mechanisms. However, their mechanism of heart rhythm remains controversial.

Methods: We investigated the role of the GABA_B receptor (GABA_BR) in mediating GLP-1RA's chronotropic and anti-arrhythmic effects in a murine myocardial infarction (MI) model. MI was induced by left anterior descending artery ligation. Cardiomyocyte-specific Gabbr1-knockout (Gabbr1^{cKO}) mice were generated via AAV9-cTnT-Cre delivery to Gabbr1^{ff} mice. Cardiac sympathetic denervation was achieved by 6-hydroxydopamine (6-OHDA) treatment and sympathectomy. Mechanistic insights were obtained through Western blotting, immunofluorescence, *in vivo* electrophysiology, and patch-clamp recordings.

Results: GLP-1RA increased the heart rate independent of the sympathetic input, suggesting a cardiac-autonomous mechanism. $GABA_BR$ activation attenuated GLP-1RA-induced tachycardia, whereas Gabrb1 deficiency exacerbated it. $GABA_BR$ agonism enhanced resistance to ventricular arrhythmias post-MI in a GLP-1RA-dependent manner. Patch-clamp analysis revealed that $GABA_BR$ -induced repolarization can be suppressed by semaglutide in a dosedependent manner, indicating the possible mechanism.

Conclusion: GABA $_B$ R activation counteracts GLP-1RA's chronotropic effects while synergistically enhancing anti-arrhythmic efficacy post-MI, highlighting a novel GABA $_B$ R/GLP-1R interaction in cardiac electrophysiology.

KEYWORDS

glucagon-like-peptide 1 receptor, GABAB receptor, heart rate, myocardial infarction, ventricular arrhythmias

1 Introduction

Glucagon-like peptide-1 receptor agonists (GLP-1RAs), the first-line drugs for type II diabetes mellitus and obesity, also improve cardiac contractility and cardiometabolism, and prevent ischemia-induced myocardial injury via coupling with the cAMP/PKA and PI3K/Akt pathways in clinical practice (Ussher and Drucker, 2023; Dang et al., 2025).

Paradoxically, GLP-1 RAs have been found to increase the heart rate (HR), which is thought to be a safety concern, as an elevated HR is an independent risk factor for cardiovascular adverse events (Hozawa et al., 2004). However, GLP-1RAs' positive chronotropic effect—particularly sinus tachycardia—remains mechanistically unresolved. The earliest speculation was that the positive chronotropic effect was secondary to a reduction in blood pressure mediated by vessel smooth muscle relaxation and sodium excretion. However, this hypothesis was dismissed because the acute increase in the HR post-GLP-1RA treatment was not accompanied with blood pressure decrease. The GLP-1RA mechanism affecting the HR is explained by the following: (I) autonomous nervous system modulation due to the compromised parasympathetic nervous activity after infusion of a GLP-1RA, exendin-4 and (II) a direct GLP-1 receptor-mediated effect on the endogenous sinoatrial pacemaker node of the heart (Lorente et al., 2000). Mounting evidence supports that GLP-1RAs increase the HR in a cardiac-autonomous manner rather than through autonomous nerve or baroreflex modulation (Jakob and Krieglstein, 1997; Woo et al., 2013; Hill et al., 2024).

The GABA_BR, which is a class C metabotropic G protein-coupled receptor, mediates slow and long-lasting neuronal synapse inhibition through indirect K+ and Ca2+ channel gating and through other second messengers such as cAMP. Central nervous (e.g., hypothalamus and nucleus tractus solitarius) GABAnergic neurons are suppressed by GLP-1R signaling, whereas GABAnergic activation has been well established to decrease the HR (Wang et al., 2001; Lu et al., 2024; Bony et al., 2013). Moreover, cloning has demonstrated high cardiac content of GABABR, which triggers inward-rectifying K+ currents (GIRK), accelerating repolarization and stabilizing membrane potential (Fortin et al., 2020; François et al., 2025). Otherwise, depletion of GABABR on cardiomyocytes prolonged the action potential duration (APD), creating electrophysiological heterogeneity that may predispose to arrhythmias (Gähwiler and Brown, 1985). Given that GLP-1R is expressed in cardiomyocytes, we hypothesize that the GLP-1R counteracts with GABABR on cardiomyocytes. To this end, we co-activated GABABR/GLP-1R and found that compared to single GLP-1RA, the post-MI ventricular arrhythmias was improved possibly via potentiation of GIRK. It is suggested that GLP-1RAs increase the HR through a cardiomyocyte-autonomous mechanism, independent of sympathetic input—challenging prior assumptions and offering novel insights into anti-arrhythmogenesis mechanism post-myocardial infarction (MI).

2 Methods

2.1 Animal and animal treatment

Our study examined male mice because male animals exhibited less variability in myocardial infarction phenotypes and showed more significant resilience to arrhythmia after treatment with GLP-1R/GABA_BR agonists. All animal experiment procedures followed the principles of the Guide for the Care and Use of Laboratory Animals published by the US National Institutes of Health (NIH publication no. 85-23, revised 1996) and were authorized by the Animal Care and Use Committee of Renmin Hospital of Wuhan University under the approval number: 20220301A. All male

Sprague-Dawley rats (8-9 weeks old) and male C57BL/6J mice (8-10 weeks old) were purchased from Shulaibao (Wuhan) Biotechnology Co., Ltd. Gabbr1 flox mice (#S-CKO-11747) were on a C57B/J background. The myocardial infarction models were induced by 6-0 suture ligation of the left anterior descending branch of the coronary artery. Sham surgery was performed in the same procedure, except for artery ligation. The success in myocardial infarction modeling is indicated by ST segment elevation from ECG. Semaglutide was injected subcutaneously at a dose of 100 µg/kg/day and treated once a day. Stellate ganglionectomy was performed on all mice under a surgical microscope, following the procedure previously reported (Hill et al., 2024). Lungs were pulled caudally to visualize stellate ganglion between the first and second rib beneath the parietal pleura. Chemical denervation was achieved via 100 mg/kg 6-hydroxydopamine (6-OHDA, diluted into 0.3% ascorbic acid) injection. Baclofen (15 mg/kg) dissolved in 0.9% saline was applied interperitoneally 1 day before semaglutide treatment. Mice were fed for another 1 week after surgery. All mice were fed in a standard environment with controlled light/dark cycles (12-h light/12-h dark), ambient temperature, and humidity. Tail-vein injection of AAV9-cTnT-Cre virus (WZ Biosciences, Inc, Shandong, China, 0.5×10^{E11} GC/pup) was performed to achieve cardiomyocyte-specific knockout of Gabbr1. All mice were grouped and sacrificed randomly, but no blind test was conducted in the animal experimental procedures.

2.2 Cell culture and cell treatment

iPSC-derived cardiomyocyte was obtained from CardioEasy (CA2201106, CellAPY, China). The cells were cultured in DMEM/F-12 (11554546, Gibco, United States), 2% B27 insulin-free (A1895601, Thermo Fisher Scientific, United States) penicillin–streptomycin (1%; 100 units/mL penicillin and 100 µg/mL streptomycin) (Cellclone; Genetix Biotech Asia Pvt. Ltd.). The cell culture incubator (Forma Steri-Cycle M, 370, Thermo Fisher, USA) was in a humidified air containing 5% $\rm CO_2$ at 37 °C. A total of $\rm 1\times10^6$ cells were seeded in a T-25 culture flask (Eppendorf, Hamburg, Germany). Each plate was seeded with an equal amount of cells.

2.3 Echocardiography

The cardiac function of mice was evaluated at 1 week after surgery with echocardiography (Visual et al., 2100, Toronto, Canada), equipped with a 23-MHz line array transducer. The mice were maintained under 0.5% anesthesia and placed in the supine position on a 37 °C heating pad. M-mode images were obtained to measure left ventricular end-systolic volume (LVESV) and left ventricular end-diastolic volume (LVEDV). Left ventricular ejection fraction (LVEF) and fractional shortening (FS) were obtained from the VEVO system.

2.4 Histopathology analysis

The hearts were fixed in 4% paraformal dehyde and sectioned into 5 $\mu m\text{-thick}$ slices. Based on the standard procedure, the

hematoxylin-eosin (HE) staining and Masson's staining in crosssection were performed to evaluate myocardial condition and fibrosis condensation. ImageJ (Fiji) was used for the calculation.

2.5 Immunofluorescence

The ventricular sections were cut into approximately $5-\mu m$ slices, followed by paraffinization, rehydration, heat-mediated antigen retrieval, and treatment with $3\%~H_2O_2$. After blocking for 1 h with 5% bovine serum, the slices were incubated with the primary antibody overnight at 4 C. Antibody information was as follows: anti-tyrosine hydroxylase (Abcam, ab6211, Germany, 1: 500) and anti-cTnT (Abcam, ab8295, Germany, 1:1000). The next day, sections were incubated with the horseradish peroxidase (HRP)-labeled secondary antibody for 2 h at 37 C. Immunofluorescence images were captured using a confocal laser scanning microscope (ZEISS LSM 800).

2.6 Electrocardiogram (ECG) and *in vivo* electrophysiology

Atrial pacing was produced through transesophageal programmed electrical stimulation. Mouse anesthesia was maintained by 1% isoflurane. Standard surface ECG was recorded using the PowerLab System (AD instruments) with a subcutaneous ECG surface (lead II). The tracheal tube was inserted into the trachea through the glottis, and the chest fluctuation of the mice was observed to be consistent with the ventilator frequency, which proved that the tracheal intubation was successful. Then, a 2.2F six-polar catheter was inserted into the esophagus near the left atrium, and correct placement was confirmed through burst waves. To correct for the HR, Bazett's formula-corrected QT interval (QTc) was used. The ECG of mice at the rest state was recorded consecutively for 5-10 min. Subsequently, sodium pentobarbital (50 mg/kg, intraperitoneal) was used to anesthetize animals. With a platinum MAP electrode and stimulation procedures, the monophasic action potentials (MAPs) of the left ventricle were recorded. The paired platinum-stimulating electrode was positioned on the basal surface of the right ventricle to deliver regular pacing. The heart was stimulated with a regular pacing cycle length (PCL). Action potential duration 90 (APD₉₀) was defined as the average repolarization time of 90% of 6-8 consecutive MAPs when the PCL was 150 ms. S1-S1 pacing was used to measure APD and activation latency time (ALT). To induce ALT, PCL was decreased, starting at 150 ms and gradually reduced by 10 ms, and then by 5 ms from 100 to 50 ms, until APD alternans occurred. Ventricular arrhythmias (VAs) were induced by burst pacing with 2 ms pulses delivered at 50 Hz for 2 s, repeated 20 times and separated by 2-s intervals. VA is defined as ventricular tachycardia (VT) or ventricular fibrillation (VF) lasting 2 s or more.

2.7 Enzyme-linked immunosorbent assay (ELISA)

Cardiac samples were homogenized in a tissue lysis buffer (pH: 7.4 with 150 mmol/L NaCl, 1% Triton $\times 100$, and proteinase

inhibitor) and centrifuged (10,000 g, 10 min, 4 °C). The supernatant was then collected, and its protein concentration was adjusted to 500 $\mu g/\mu L$. Commercial ELISA kits were used to detect the norepinephrine level (ab287789, Abcam, USA).

2.8 Patch clamp recording

A soft glass capillary pulled to a tip resistance of 1.5–2 M Ω (Sutter Instruments, Novato, CA) was used for whole-cell patch clamp. Signals were recorded using an Axopatch 200A (Axon Instruments, Foster City, CA) with a computer-interacted 125-kHz Labmaster board (Axon Instruments). Membrane currents were sampled at 1–2 kHz and filtered at 2 kHz. Series resistance ($R_{\rm s}=7.0\pm1.0~{\rm M}\Omega$) was compensated by \approx 80%. Cells to be tested were incubated at 35 °C in the bath solution supplemented with 300 ng/mL pertussis toxin for 4 h. The buffer was supplemented with 2 mM Co²⁺ and 3 mM 4-aminopyridine to block transient rectifying current and calcium current. Voltage commands, data acquisition, and analysis were performed using pClamp 6.0.

2.9 Western blotting (WB) analysis

The tissue samples were lysed in $1\times$ RIPA buffer (G2002, ServiceBio, Wuhan, China). Subsequently, protein samples were separated using SDS-PAGE and then transferred into the PVDF membrane (IPVH00010, Merk Millipore, Germany). After the PVDF membranes were blocked with 5% fat-free bovine milk for 2 h, specific primary antibodies were incubated overnight at 4 °C. The primary antibodies included. The next day, the membranes were incubated with HRP-conjugated goat anti-rabbit secondary antibodies (ServiceBio, Wuhan, China) for 1 h. Finally, protein bands were visualized through enhanced chemiluminescence (BL523B, Biosharp, China). Antibody information was as follows: anti- α SMA (1:1000, Cell Signaling Technology, United Kingdom, #19245) and anti-TGF- β (1:1000, Cell Signaling Technology, United Kingdom, #3711).

2.10 Statistical analysis

All statistical analyses were performed using GraphPad Prism 8.0 (Inc., La Jolla, CA, USA). Data are presented as mean \pm SD. Statistical analyses used repeated two-way ANOVA and paired Student's *t*-tests where appropriate (*p* <0.05). Values were considered statistically significant when P < 0.05.

3 Results

3.1 GLP-1RA-mediated cardiac positive chronotropic effect is possibly not neuronal-dependent

GLP-1R is highly enriched in autonomous neurons and cardiomyocytes. To investigate whether the autonomous nervous system is sufficient for mediating GLP-1RA-related fast pacing

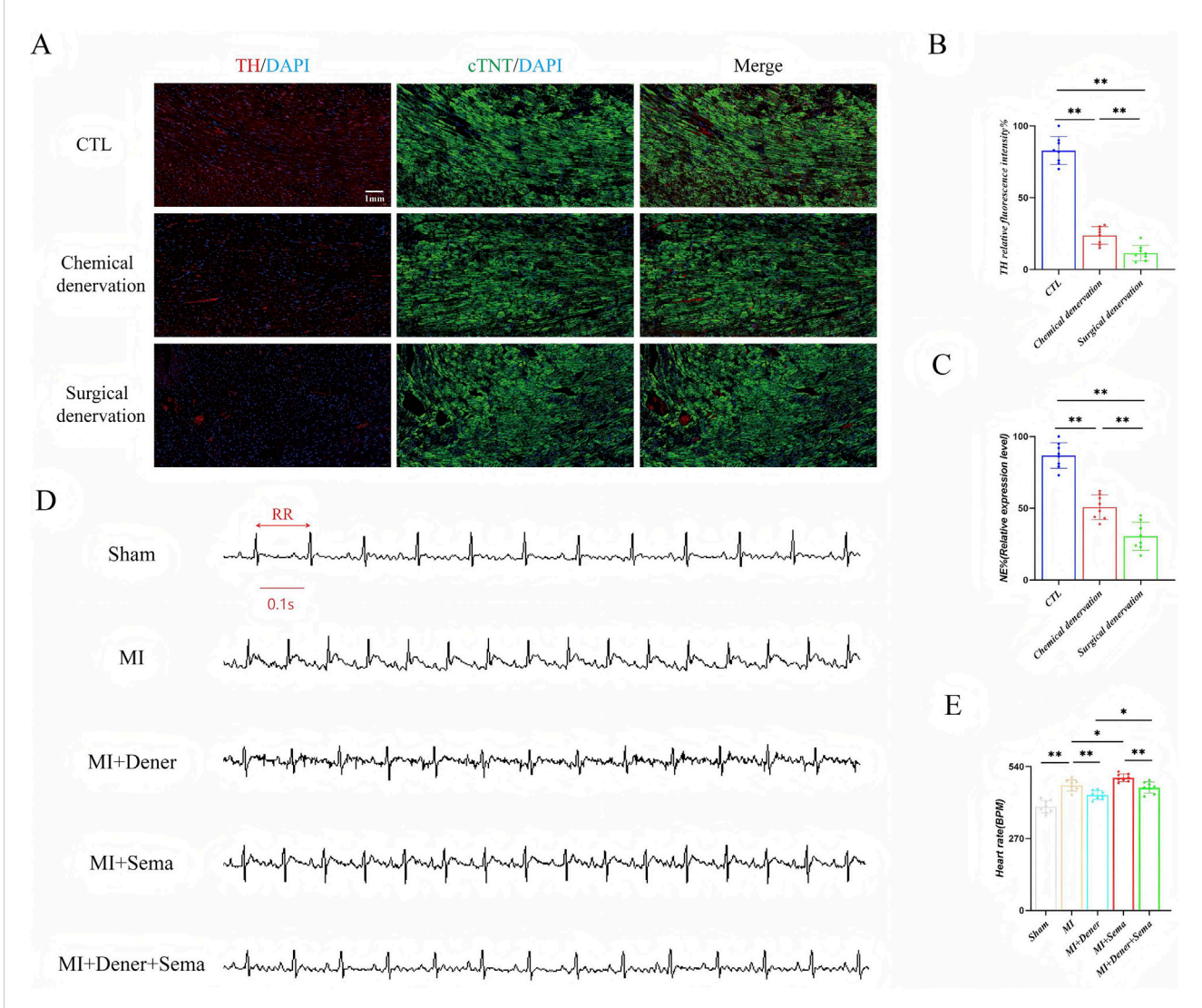
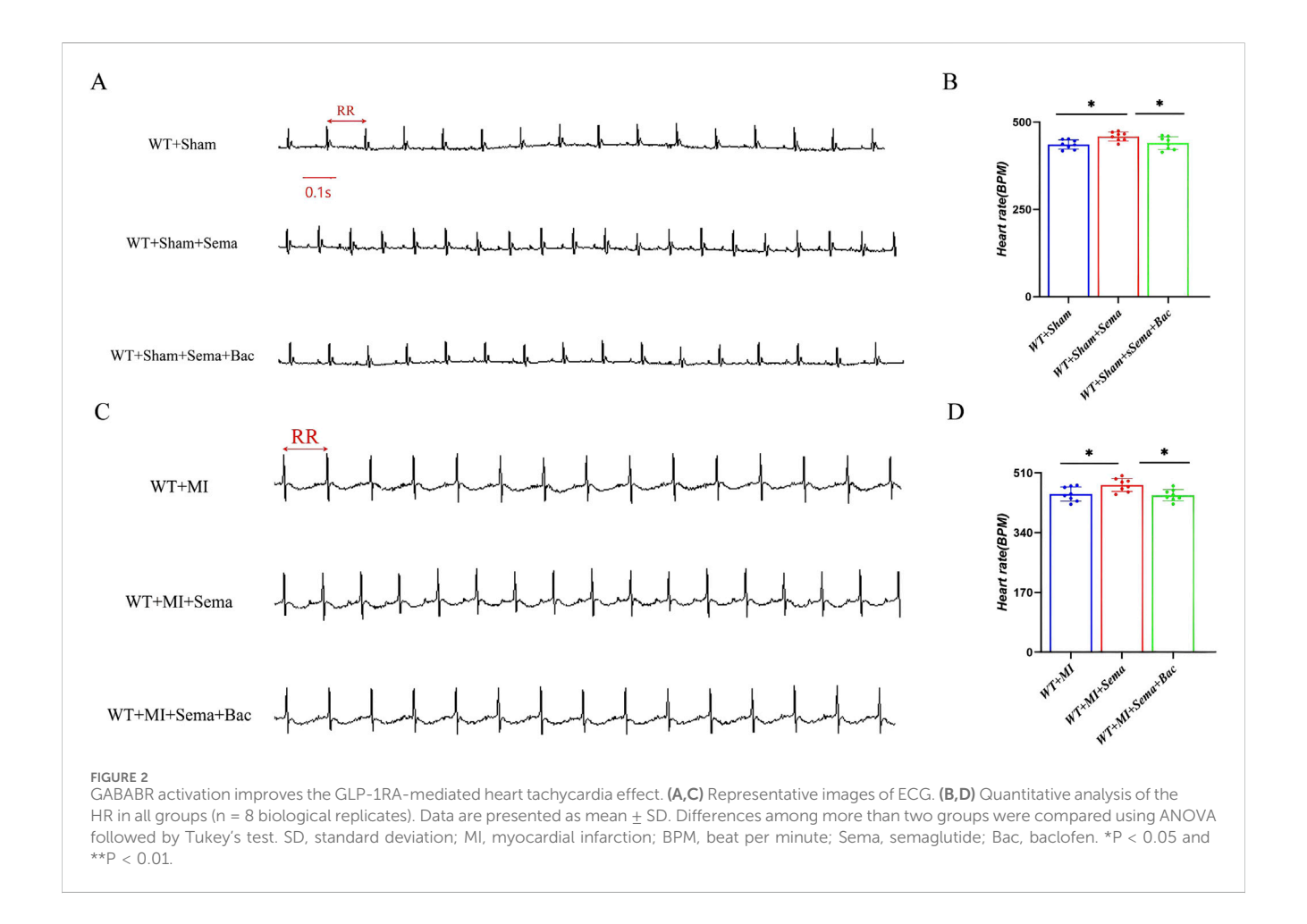


FIGURE 1
GLP-1RA-mediated cardiac positive chronotropic effect is possibly not neuronal-dependent. (A) The representative images of tyrosine hydroxylase immunofluorescent staining. (B) Quantitative analysis of relative tyrosine hydroxylase positive rate in all groups (n = 8 biological replicates). (C) Quantitative analysis of relative norepinephrine expression levels in all groups (n = 8 biological replicates). (D) Representative images of ECG. (E) Quantitative analysis of the HR in all groups (n = 8 biological replicates). Data are presented as mean ± SD. Differences among more than two groups were compared using ANOVA, followed by Tukey's test. SD, standard deviation; CTL, control; MI, myocardial infarction; TH, tyrosine hydroxylase; cTNT: cardiac troponin; NE, norepinephrine; Dener, denervation; Sema, semaglutide; BPM, beat per minute. *P < 0.05 and **P < 0.01.

effect, we blocked cardiac sympathetic innervation via 6-OHDA infusion and surgical sympathectomy. 6-OHDA, a neurotoxic agent that degrades sympathetic nerve terminals, reduced nearly 75% of tyrosine hydroxylase (TH, a key enzyme involved in the production of norepinephrine) fluorescence signals in cardiac tissue, and bilateral stellate sympathectomy depleted 87% of TH+ signals (Figures 1A,B). The indicator of sympathetic innervation, norepinephrine, was also significantly reduced after both 6-OHDA infusion and sympathectomy, as determined by ELISA (Figure 1C). Semaglutide treatment increased the HR to a new baseline, whereas heart denervation did not lead to further change in the HR, which suggests that the autonomous nervous system might not be sufficient for GLP-1RA's positive chronotropic effect (Figures 1D,E).

3.2 GABA_BR activation improves the GLP-1RA-mediated heart tachycardia effect

GABA_BR was identified as a direct binding partner of GLP-1R in a previous biotin proximity labeling screen (Dang et al., 2025). To validate the function of the GABA_BR/GLP-1R interaction, pharmacological activation of GABA_BR with baclofen, a GABA-mimetic GABA_BR agonist, prior to MI induction, reduced the chronotropic effect of semaglutide under physiological conditions (Figures 2A–D). However, the activation of GABA_BR did not accelerate the HR under physiological conditions (Supplementary Figure S1). Moreover, this antagonistic effect of GLP-1RA and GABA_BR on the HR was preserved in post-MI mice. Here, we hypothesize



that $GABA_BR$ serves as an antagonizing mediator for GLP-1R regarding HR modulation, potentially through direct receptor cross-talk or intracellular downstream.

3.3 GLP-1R collaborates with GABA_BR to increase the resilience to post-myocardial infarction ventricular arrhythmia

To determine whether the baclofen-induced reduction in the HR depends on GLP-1R signaling, we generated cardiac GABABR-knockout (Gabbr1cKO) mice by injecting AAV9cTnT-Cre into Gabbr1ff mice and assessed cardiac electrophysiology in vivo (Supplementary Figure S2). Gabbr1 encodes an essential subunit required for GABABR activation. As shown in Figures 3A,B, dual treatment with GLP-1RA and baclofen significantly shortened the action potential duration at APD90 (MAPs, 150 ms) in wild-type mice. This effect was abolished in Gabbr1^{cKO} mice and in those receiving monotherapy with either semaglutide or baclofen (Figures 3G,H). We next evaluated the ALT in the left ventricle by S1-S1 pacing. In Gabbr1-intact mice (Figures 3C,D), combined semaglutide and baclofen treatment attenuated MIinduced ALT prolongation. In contrast, no changes in ALT were observed in Gabbr1ckO mice under either monotherapy or combination therapy (Figures 31,J). To further assess arrhythmic susceptibility, we performed burst pacing (Figures 3E,F). In Gabbr1^{f/f} mice, co-administration of GLP-1RA and baclofen reduced both the incidence and duration of post-MI ventricular arrhythmias. However, in *Gabbr1*^{cKO} mice, dual GLP-1R/GABA_BR activation failed to confer anti-arrhythmic protection (Figures 3K,L). Collectively, these findings demonstrate that GABA_BR activation is required for the anti-arrhythmic effects of GLP-1RAs.

3.4 GABA_BR is required for the cardiac function improvement relative to GLP1RA

To determine whether dual activation of GABABR and GLP-1R further improves cardiac function, we performed echocardiography in *Gabbr1*^{fif} and *Gabbr1*^{cKO} mice after MI. In wild-type mice, GLP-1RA administration improved post-MI cardiac performance, as reflected by increased LVEF and LVFS and reduced LVESV and LVEDV (Figures 4A,C). In contrast, *Gabbr1*^{cKO} mice failed to show any improvement in cardiac function or survival following GLP-1RA treatment (Figures 4B,D). Moreover, GLP-1RA reduced the 30-day post-MI mortality rate in wild-type mice, whereas this benefit was abolished in *Gabbr1*^{cKO} mice (Figures 4E,F). Together, these results indicate that GABABR activation is essential for the cardioprotective and survival benefits of GLP-1RA therapy after MI.

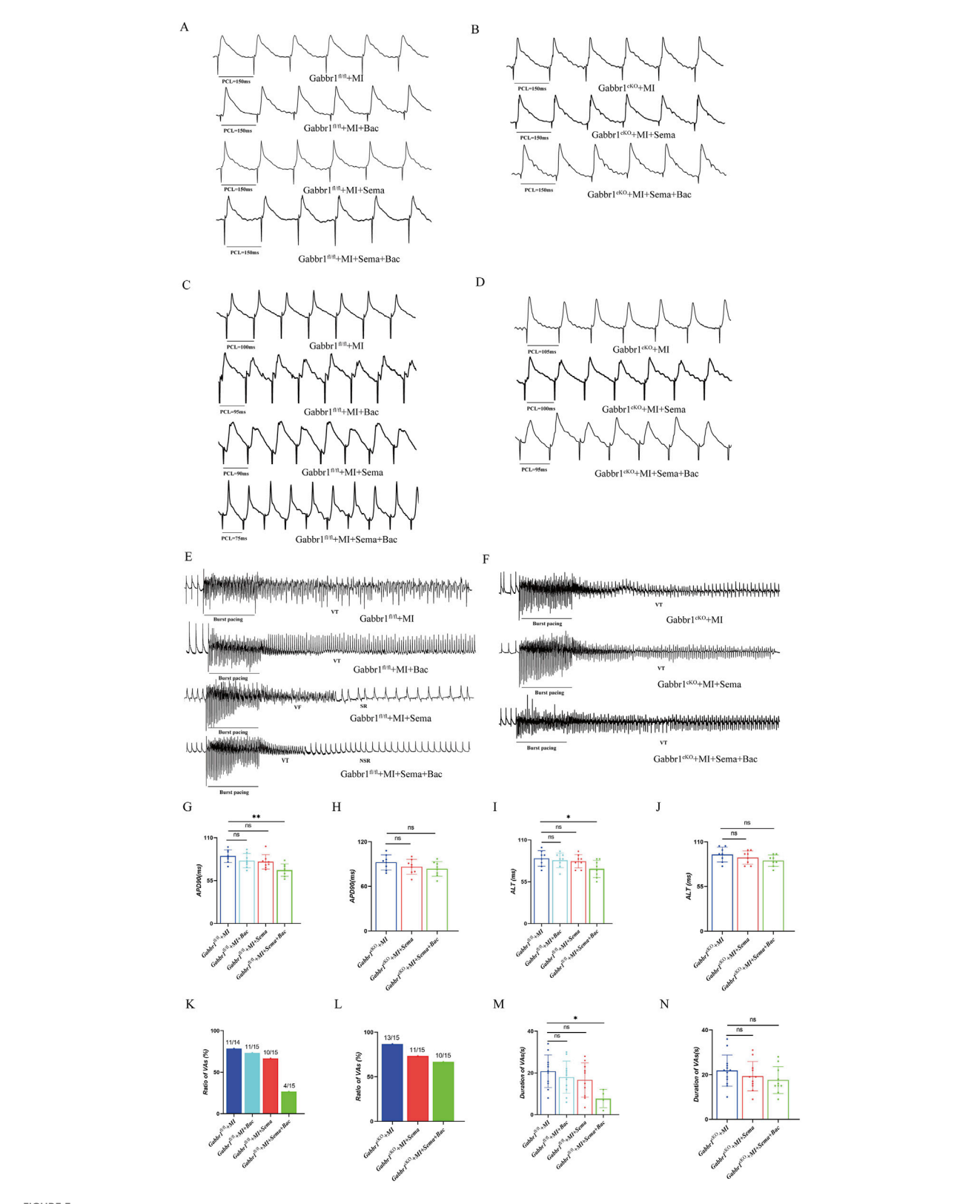
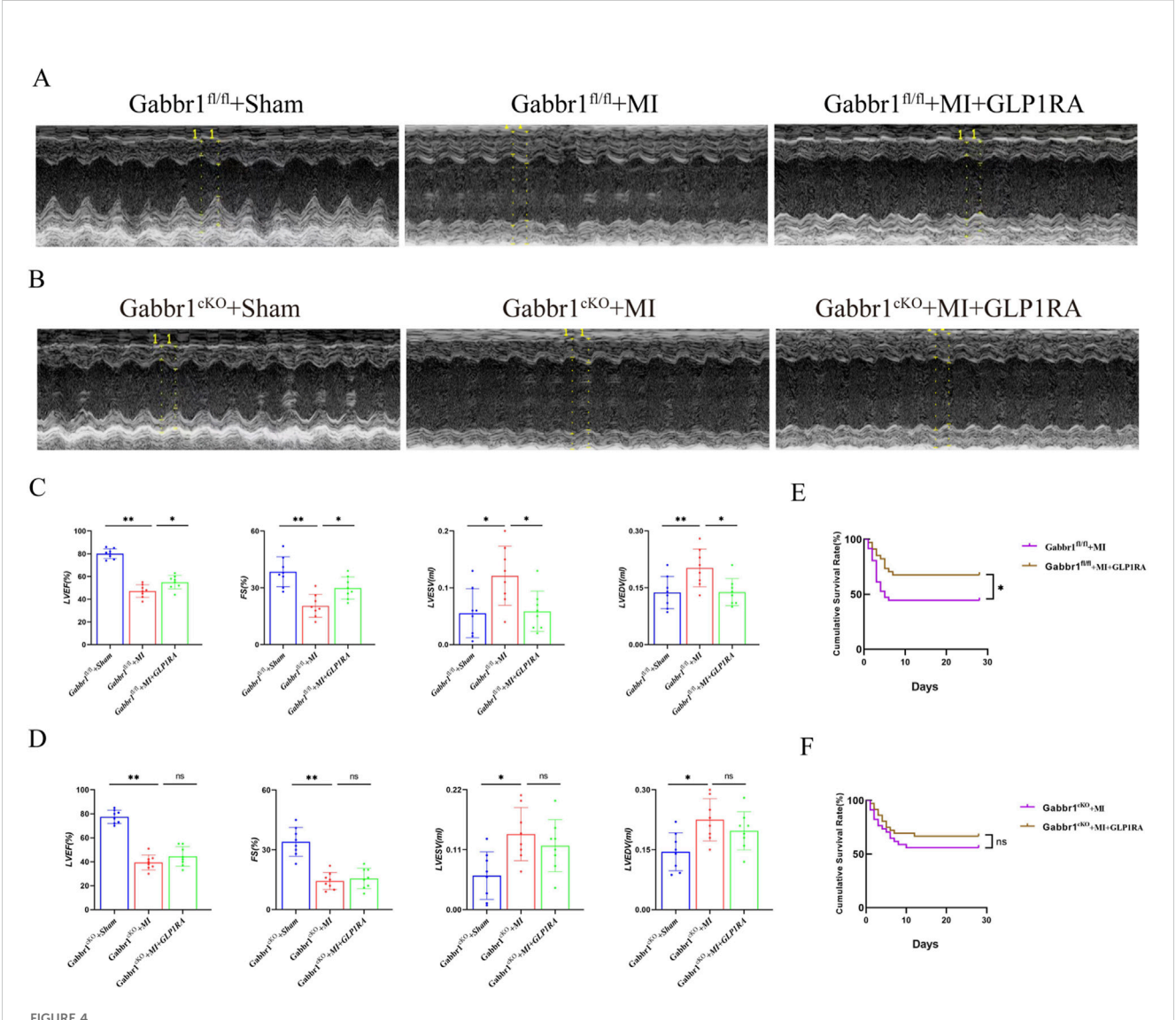


FIGURE 3
GLP-1R collaborates with GABABR to increase the resilience to post-myocardial infarction ventricular arrhythmia. (A,B) Representative images of the MAP recordings at a PCL of 150 ms; (C,D) representative images of the MAP recordings of ALT; (E,F) representative images of the MAP recordings after burst pacing; (G,H) quantitative analysis of APD90 at 150 ms PCL in all groups (n = 8 biological replicates); (I,J) quantitative analysis of the threshold interval for ALT in all groups (n = 8 biological replicates); (K,L) quantitative analysis of VA inducibility in all groups (n = 14–15 biological replicates); (M,N) quantitative analysis of duration of ventricular arrhythmias in all groups. MAP, monophasic action potentials; PCL, pacing cycle length; VAs, (Continued)

FIGURE 3 (Continued)

ventricular arrhythmias. Data are presented as mean \pm SD. Differences among more than two groups were compared using ANOVA followed by Tukey's test. SD, standard deviation; Sema, semaglutide; Bac, baclofen; VT, ventricular tachycardia; VF, ventricular fibrillation; SR, sinus rhythm; NSR, normal sinus rhythm. *P < 0.05 and **P < 0.01.



GABABR cardiomyocyte knockout counteracts cardiac dysfunction relative to GLP-1RA. (A,B) Representative images of left ventricular M-mode echocardiographic recordings. (C,D) Quantitative analysis of cardiac function by LVEF (%), LVFS (%), LVEDV (mL), and LVESV (mL) in all groups (n = 8 biological replicates). (E,F) Kaplan-Meier survival curves of the MI group and MI + GLP-1RA group mice 4 weeks after MI (n = 34 per group). Data are presented as mean \pm SD. Differences among more than two groups were compared using ANOVA followed by Tukey's test. SD, standard deviation. *P < 0.05 and **P < 0.01.

3.5 GABA_BR/GLP-1R signaling has no acute effect on fibrosis

To further assess the role of GABA_BR/GLP-1R dual activation in post-infarction remodeling, we examined cardiac fibrosis using Masson's trichrome and HE staining. *Gabbr1* deficiency did not alter the cardiac morphology or structure after MI, regardless of treatment with semaglutide alone or in combination with baclofen (Figures 5A,B). Quantitative analysis showed no significant differences in collagen deposition or infarct size with GLP-1RA

treatment, either alone or with GABA_BR co-activation (Figures 5C,D), indicating that neither GLP-1R nor GABA_BR activation confers acute antifibrotic benefit. Consistently, Western blotting of left ventricular tissue revealed no changes in α -smooth muscle actin (α -SMA, a marker of myofibroblast activation) or transforming growth factor- β (TGF- β , a pro-fibrotic marker) in either wild-type (Figures 5E,G) or $Gabbr1^{cKO}$ mice (Figures 5F,H). Collectively, these findings suggest that acute GABA_BR/GLP-1R activation does not significantly modulate cardiac fibrosis progression after MI.

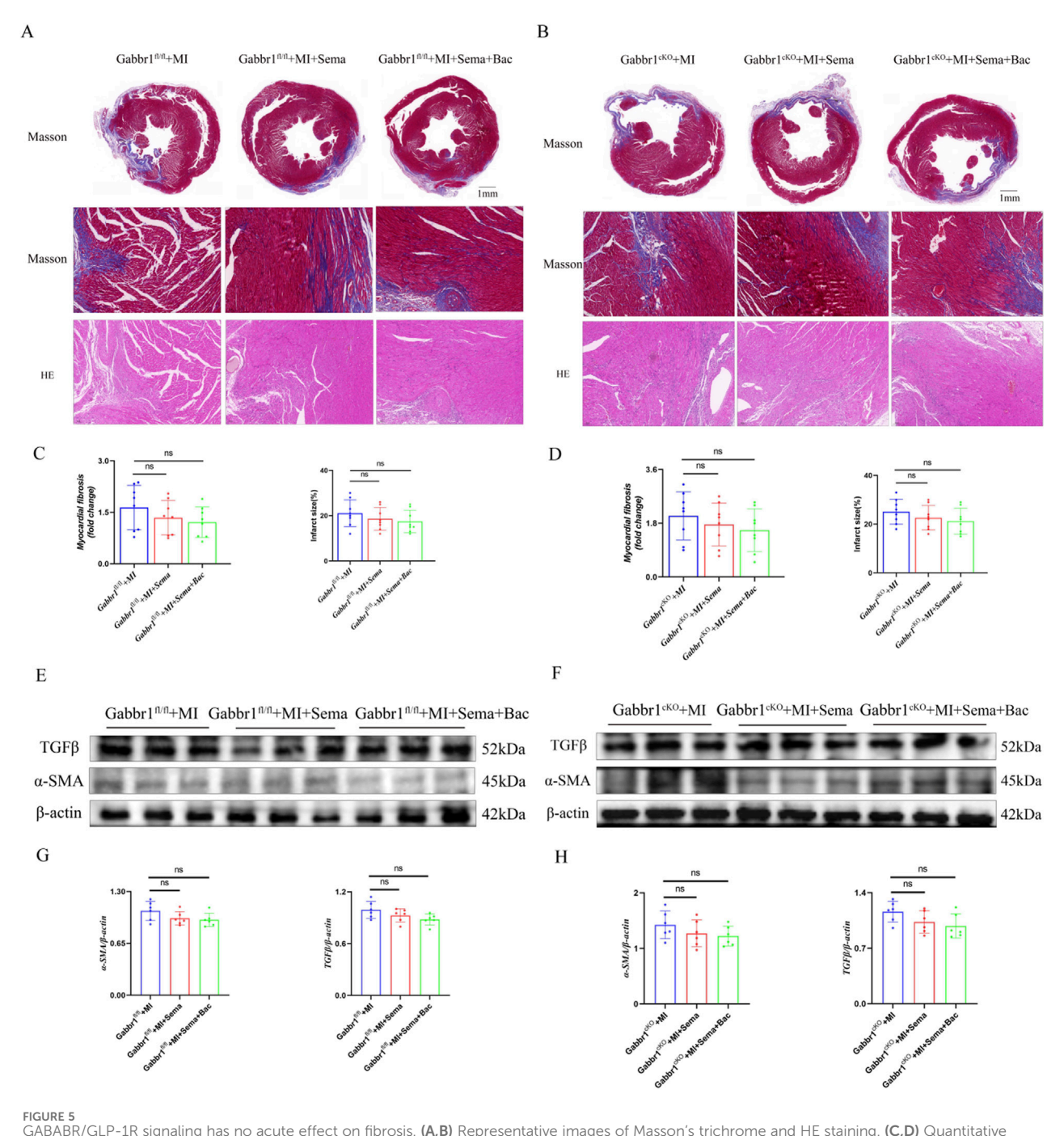
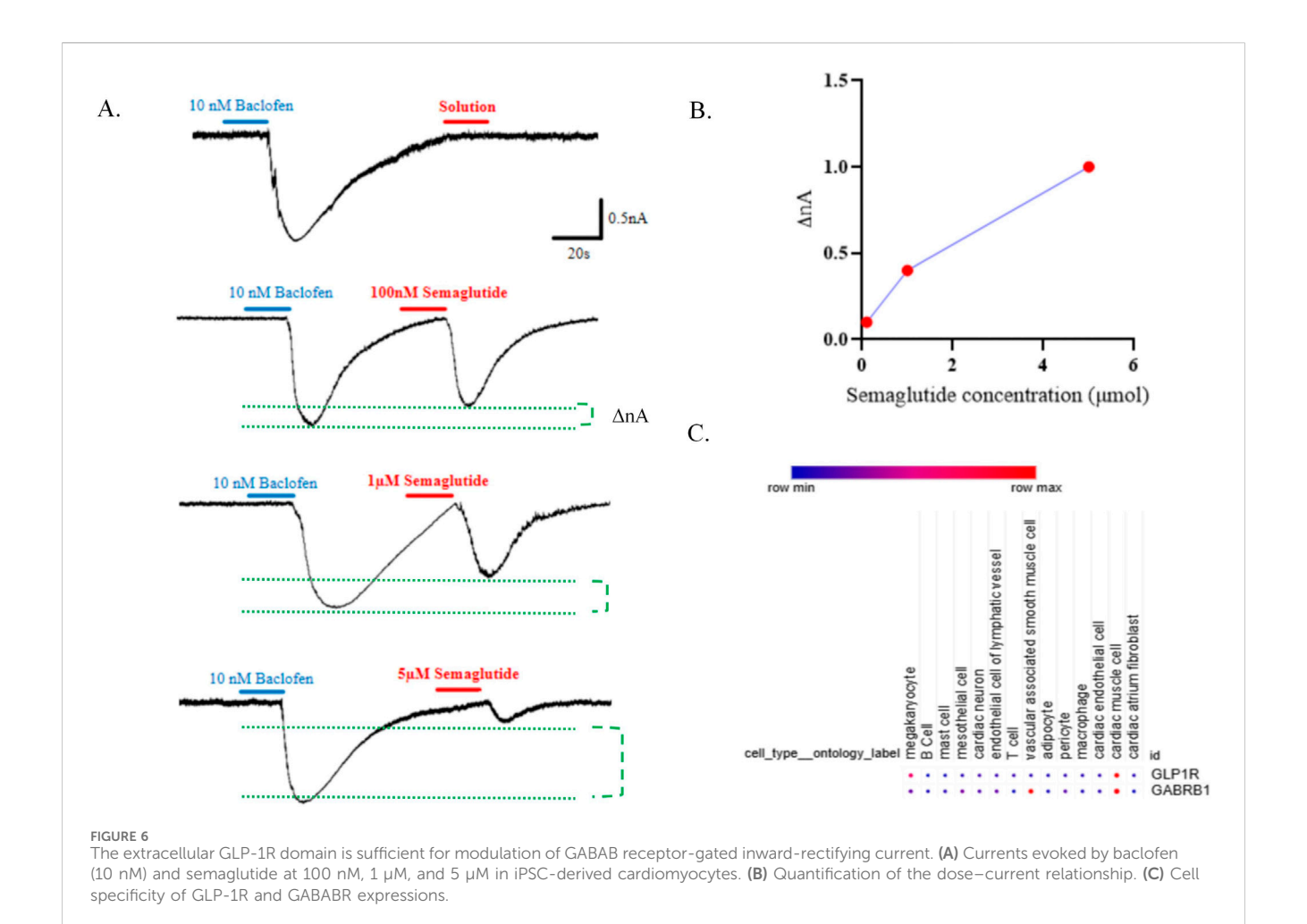


FIGURE 5 GABABR/GLP-1R signaling has no acute effect on fibrosis. (A,B) Representative images of Masson's trichrome and HE staining. (C,D) Quantitative analysis of relative fibrosis area in the groups (n = 8 biological replicates); (E–H) Representative Western blotting bands and quantitative analysis of α -SMA and TGF β in all groups (n = 8 biological replicates). Data are presented as mean \pm SD. Differences among more than two groups were compared using ANOVA followed by Tukey's test. SD, standard deviation; MI, myocardial infarction; Sema, semaglutide; Bac, baclofen *P < 0.05 and **P < 0.01.

3.6 GABA_BR-induced inward-rectifying current is inhibited by GLP-1RA

 ${\rm GABA_BR}$ activation enhances potassium conductance through inwardly rectifying GIRK channels in a G protein-dependent manner, and baclofen is sufficient to induce this current. To assess whether GLP-1RAs modulate ${\rm GABA_BR}$ -mediated inward currents, we performed whole-cell patch-clamp recordings in

hiPSC-derived cardiomyocytes. Baclofen evoked inward currents, which were suppressed by GLP-1R activation in a concentration-dependent manner (Figures 6A,B). In addition, re-analysis of single-cell RNA sequencing data from cardiac tissue of 46 arrhythmia patients (Matthew C. Hill et al.) revealed co-expression of GABABR and GLP-1R in cardiomyocytes (Figure 6C) (Marso et al., 2016). Together, these findings suggest that GLP-1RAs attenuate GABABR-gated depolarizing currents in cardiomyocytes.



4 Discussion

The positive chronotropic effect of GLP-1RAs are well documented, yet their mechanism remains elusive (Yang et al., 2024; Lu et al., 2023). To determine whether GLP-1RA acts via neural-dependent or neural-independent pathways is critical for optimizing GLP-1RA usage in cardiac ischemic diseases. Although neuronal GLP-1R is concentrated in autonomous neuron axons and synaptic regions, cardiomyocyte autonomous GLP-1R appears to work independently. Our study demonstrated that sympathetic denervation did not abolish the GLP-1RA-mediated modulation of the HR in MI mice. This contrasts with previous models attributing GLP-1RA-induced tachycardia to the autonomous nervous system as our findings suggest an cardiomyocyte-expressed GABA_BR-involved mechanism.

GABA_BR signals via G-proteins and is localized at pre- and post-synaptic sites. Presynaptic GABA_BRs couple to Ca²⁺ channels to regulate neurotransmitter release, whereas postsynaptic GABA_BRs activate inwardly rectifying K⁺ (Kir3) channels, mediating slow inhibitory currents (Lorente et al., 2000; Fortin et al., 2020). Our data indicate that postsynaptic GABA_BRs in cardiomyocytes interact with GLP-1R to modulate spontaneous membrane potential, implicating a potential antiarrhythmic role following cardiac ischemia. The interaction between GLP-1R and GABA_BR has also been characterized in the central nervous

system. For instance, GLP-1R knockout in the nucleus tractus solitarius attenuates GABAergic signaling, reducing food intake and body weight (Jagomäe et al., 2025). Additionally, local liraglutide administration suppresses postsynaptic GABA receptor activity while enhancing presynaptic GABAergic neuron firing (Maitre et al., 1983). These findings suggest that GLP-1R signaling modulates GABA receptor function. Notably, both γ-hydroxybutyrate, a GABA analog, and the GABA_BR agonist baclofen induce dose-dependent hyperpolarization via Kir channel-mediated K+ efflux, supporting functional GABABR expression in cardiomyocytes (Dauvilliers et al., 2022; Ast et al., 2023). To further validate this mechanism, we generated cardiomyocyte-specific GABA_BR-knockout models. Intriguingly, GABA_BR deletion led to GLP-1R-mediated HR elevation, whereas GABA_BR activation with baclofen reduced the HR. These findings suggest a neural-independent mechanism by which GLP-1R-GABA_BR interaction regulates cardiac electrophysiology.

So far, the therapeutic potential of GLP-1RAs in ischemic myocardium has been debated. Although some clinical trials reported a reduced myocardial injury biomarkers and modest improvements in left ventricular ejection fraction, others showed no significant outcome benefits. Furthermore, GLP-1RA-induced tachycardia may increase myocardial oxygen demand, potentially offsetting metabolic benefits in acute ischemia. Our data propose that selectively blocking GLP-1R-mediated chronotropic effects via

agonizing GABA_BR might expand GLP-1RA utility into acute coronary syndromes. In addition, the effect of GLP-1RA on the HR is consistent at both the early phase (autonomic overdrive) and late phase (recovered innervation) of MI, further supporting the phenomenon of autonomous nerve independence. GLP-1RA is believed to mediate intracellular signaling through Gas, thus activating subsequent adenylate cyclase and increasing the cAMP level (Durak and Turan, 2023). As a result, protein kinase A is activated. Acute cAMP/PKA enhancement can mediate the positive chronotropic effect and attenuation of calcium entrance and RyR2 phosphorylation to cause arrhythmogenesis (Younce et al., 2013; Yaniv et al., 2015). Meanwhile, the cAMP/PKA cascade is positioned in the negative regulation of adenylate cyclase by GABA_BR (Lubberding et al., 2024). Otherwise, after GABABR activates inward-rectifying channels, the outward K+ current increases, leading to hyperpolarization of sinoatrial node cells and counteracting the depolarization caused by GLP-1R through HCN channels (If current) to reduce the pacing frequency. Moreover, inhibiting the action potential increasing rate via activation of L-type calcium channels (I_{Ca-L}) could also contribute to this effect (Lüscher et al., 1997).

GLP-1R agonists, whether administered centrally or peripherally, can increase the HR in rodents (Wei and Mojsov, 1995; Wei and Mojsov, 1996; Bullock et al., 1996), induce the expression of c-Fos in adrenal medullary catecholamine neurons, and activate tyrosine hydroxylase in the brainstem. We believe these data suggest that some of the rapid cardiovascular effects of GLP-1 may be due to the increased outflow of catecholamines in the brain and elevated sympathetic nerve tension. Under physiological conditions, GLP-1RA's fast HR effect can be dominated by the autonomous tone. However, under denervating conditions, cardiomyocyte-autonomous GLP-1R can also be a compensative mechanism under the assistance of some co-receptors, such as GABA_BR. However, a previous study by Lubberding et al. showed that denervation could not abolish the regulation of GLP-1RA on the HR (Lubberding et al., 2024), which is consistent with our findings. There are some limitations to our work. The distribution pattern of GLP-1R differs between mice and humans, which may result in a difference in the mechanism, as GLP-1R in humans is more expressed on cardiomyocytes, whereas Glp-1r in mice is expressed more on endothelial-like cells from single-cell data (McLean et al., 2022). We have yet to consider the expression pattern of GLP-1R between human and mice, which may limit the clinical relevance. Our study focuses on the overall effect of GLP-1RA without GLP-1 analogs for a positive control and provides no evidence to illustrate that the vascular expressed Glp-1r is not important for the chronotropic effect and anti-arrhythmia potential of Gababr/Glp-1r dual agonization. Finally, baclofen, administered 1 day before semaglutide, likely has central effects (and residual sedation) with a half-life of approximately 3 h. The HR was measured under isoflurane, which can also depress heart beating and modulate the autonomic tone. In the future, whether GLP1 directly synergizes with GABABR activation or GLP-1R activation sensitizes GABABR signaling remains to be tested. The relationship between postsynaptic GLP-1R activation and presynaptic GABA release requires further exploration.

Overall, our findings identified a novel cardioprotective axis, where GLP-1R-GABA $_{\rm B}$ R cross-talk fine-tunes cardiac electrophysiology, and under denervating conditions, cardiomyocyte GLP-1R can also be a compensative mechanism under the assistance of some chaperones such as GABA $_{\rm B}$ R.

Data availability statement

The original contributions presented in the study are included in the article/Supplementary Material, further inquiries can be directed to the corresponding authors.

Ethics statement

The animal study was approved by the Animal Care and Use Committee of Renmin Hospital of Wuhan University. The study was conducted in accordance with the local legislation and institutional requirements.

Author contributions

RQ: Formal analysis, Methodology, Project administration, Data curation, Conceptualization, Software, Investigation, Resources, original draft, Visualization. ZJ: Software, Conceptualization, Methodology, Visualization, Investigation, Writing - review and editing, Resources, Project administration. GH: Investigation, Methodology, Software, Conceptualization, Writing - review and editing, Project administration. LC: Data curation, Writing - review and editing, Validation, Funding acquisition. HH: Methodology, Software, Formal analysis, Writing - review and editing. LJ: Writing - review and editing, Software, Resources, Visualization, Methodology. ZY: Supervision, Formal analysis, Conceptualization, Writing - review and editing, Writing - original draft, Methodology, Software, Visualization, Investigation, Validation, Resources, Data curation. WX: Validation, Funding acquisition, Writing - review and editing, Investigation, Resources, Formal analysis, Methodology, Project administration, Data curation, Software, Visualization, Writing - original draft, Conceptualization.

Funding

The author(s) declare that financial support was received for the research and/or publication of this article. This work was supported by grants from the Open Foundation of Hubei Key Laboratory of Biological Targeted Therapy (202409) and the National Natural Science Foundation of China (No. 81600288).

Conflict of interest

The authors declare that the research was conducted in the absence of any commercial or financial relationships that could be construed as a potential conflict of interest.

Generative Al statement

The author(s) declare that Generative AI was used in the creation of this manuscript. Grammarly was used to check grammar mistakes.

Any alternative text (alt text) provided alongside figures in this article has been generated by Frontiers with the support of artificial intelligence and reasonable efforts have been made to ensure accuracy, including review by the authors wherever possible. If you identify any issues, please contact us.

Publisher's note

All claims expressed in this article are solely those of the authors and do not necessarily represent those of their affiliated

organizations, or those of the publisher, the editors and the reviewers. Any product that may be evaluated in this article, or claim that may be made by its manufacturer, is not guaranteed or endorsed by the publisher.

Supplementary material

The Supplementary Material for this article can be found online at: https://www.frontiersin.org/articles/10.3389/fphar.2025.1616181/full#supplementary-material

References

Ast, J., Nasteska, D., Fine, N. H. F., Nieves, D. J., Koszegi, Z., Lanoiselée, Y., et al. (2023). Revealing the tissue-level complexity of endogenous glucagon-like peptide-1 receptor expression and signaling. *Nat. Commun.* 14 (1), 301. doi:10.1038/s41467-022-35716-1

Bony, G., Szczurkowska, J., Tamagno, I., Shelly, M., Contestabile, A., and Cancedda, L. (2013). Non-hyperpolarizing GABAB receptor activation regulates neuronal migration and neurite growth and specification by cAMP/LKB1. *Nat. Commun.* 4, 1800. doi:10. 1038/ncomms2820

Bullock, B. P., Heller, R. S., and Habener, J. F. (1996). Tissue distribution of messenger ribonucleic acid encoding the rat glucagon-like peptide-1 receptor. *Endocrinology* 137 (7), 2968–2978. doi:10.1210/endo.137.7.8770921

Dang, T., Yu, J., Cao, Z., Zhang, B., Li, S., Xin, Y., et al. (2025). Endogenous cell membrane interactome mapping for the GLP-1 receptor in different cell types. *Nat. Chem. Biol.* 21, 256–267. doi:10.1038/s41589-024-01714-1

Dauvilliers, Y., Bogan, R. K., Šonka, K., Partinen, M., Foldvary-Schaefer, N., and Thorpy, M. J. (2022). Calcium, magnesium, potassium, and sodium oxybates oral solution: a lower-sodium alternative for cataplexy or excessive daytime sleepiness associated with narcolepsy. *Nat. Sci. Sleep.* 14, 531–546. doi:10.2147/NSS.279345

Durak, A., and Turan, B. (2023). Liraglutide provides cardioprotection through the recovery of mitochondrial dysfunction and oxidative stress in aging hearts. *J. Physiol. Biochem.* 79 (2), 297–311. doi:10.1007/s13105-022-00939-9

Fortin, S. M., Lipsky, R. K., Lhamo, R., Chen, J., Kim, E., Borner, T., et al. (2020). GABA neurons in the nucleus tractus solitarius express GLP-1 receptors and mediate anorectic effects of liraglutide in rats. *Sci. Transl. Med.* 12 (533), eaay8071. doi:10.1126/scitranslmed.aay8071

Francois, M., Kaiser, L., He, Y., Xu, Y., Salbaum, J. M., Yu, S., et al. (2025). Leptin receptor neurons in the dorsomedial hypothalamus require distinct neuronal subsets for thermogenesis and weight loss. *Metabolism* 163, 156100. doi:10.1016/j.metabol.2024. 156100

Gähwiler, B. H., and Brown, D. A. (1985). GABAB-receptor-activated K+ current in voltage-clamped CA3 pyramidal cells in hippocampal cultures. *Proc. Natl. Acad. Sci. U.* S. A. 82 (5), 1558–1562. doi:10.1073/pnas.82.5.1558

Hill, M. C., Simonson, B., Roselli, C., Xiao, L., Herndon, C. N., Chaffin, M., et al. (2024). Large-scale single-nuclei profiling identifies role for ATRNL1 in atrial fibrillation. *Nat. Commun.* 15 (1), 10002. doi:10.1038/s41467-024-54296-w

Hozawa, A., Ohkubo, T., Kikuya, M., Ugajin, T., Yamaguchi, J., Asayama, K., et al. (2004). Prognostic value of home heart rate for cardiovascular mortality in the general population: the ohasama study. *Am. J. Hypertens.* 17 (11 Pt 1), 1005–1010. doi:10.1016/j. amjhyper.2004.06.019

Jagomäe, T., Velling, S., Tikva, T. B., Maksimtšuk, V., Gaur, N., Reimets, R., et al. (2025). GABA and GLP-1 receptor agonist combination therapy modifies diabetes and langerhans islet cytoarchitecture in a rat model of Wolfram syndrome. *Diabetol. Metab. Syndr.* 17 (1), 82. doi:10.1186/s13098-025-01651-6

Jakob, R., and Krieglstein, J. (1997). Influence of flupirtine on a G-protein coupled inwardly rectifying potassium current in hippocampal neurones. *Br. J. Pharmacol.* 122 (7), 1333–1338. doi:10.1038/sj.bjp.0701519

Lorente, P., Lacampagne, A., Pouzeratte, Y., Richards, S., Malitschek, B., Kuhn, R., et al. (2000). gamma-aminobutyric acid type B receptors are expressed and functional in Mammalian cardiomyocytes. *Proc. Natl. Acad. Sci. U. S. A.* 97 (15), 8664–8669. doi:10. 1073/pnas.97.15.8664

Lu, M. F., Fu, Q., Qiu, T. Y., Yang, J. H., Peng, Q. H., and Hu, Z. Z. (2023). The CaMKII-dependent phosphorylation of GABAB receptors in the nucleus accumbens

was involved in cocaine-induced behavioral sensitization in rats. CNS Neurosci. Ther. 29 (5), 1345–1356. doi:10.1111/cns.14107

Lu, Y., Wang, L., Luo, F., Savani, R., Rossi, M. A., and Pang, Z. P. (2024). Dorsolateral septum GLP-1R neurons regulate feeding *via* lateral hypothalamic projections. *Mol. Metab.* 85, 101960. doi:10.1016/j.molmet.2024.101960

Lubberding, A. F., Veedfald, S., Achter, J. S., Nissen, S. D., Soattin, L., Sorrentino, A., et al. (2024). Glucagon-like peptide-1 increases heart rate by a direct action on the sinus node. *Cardiovasc Res.* 120 (12), 1427–1441. doi:10.1093/cvr/cvae120

Lüscher, C., Jan, L. Y., Stoffel, M., Malenka, R. C., and Nicoll, R. A. (1997). G protein-coupled inwardly rectifying K+ channels (GIRKs) mediate postsynaptic but not presynaptic transmitter actions in hippocampal neurons. *Neuron* 19 (3), 687–695. doi:10.1016/s0896-6273(00)80381-5

Maitre, M., Cash, C., Weissmann-Nanopoulos, D., and Mandel, P. (1983). Depolarization-evoked release of gamma-hydroxybutyrate from rat brain slices. *J. Neurochem.* 41 (1), 287–290. doi:10.1111/j.1471-4159.1983.tb11843.x

Marso, S. P., Bain, S. C., Consoli, A., Eliaschewitz, F. G., Jódar, E., Leiter, L. A., et al. (2016). Semaglutide and cardiovascular outcomes in patients with type 2 diabetes. N. $Engl.\ J.\ Med.\ 375\ (19),\ 1834–1844.\ doi:10.1056/NEJMoa1607141$

McLean, B. A., Wong, C. K., Kabir, M. G., and Drucker, D. J. (2022). Glucagon-like Peptide-1 receptor Tie2+ cells are essential for the cardioprotective actions of liraglutide in mice with experimental myocardial infarction. *Mol. Metab.* 66, 101641. doi:10.1016/j. molmet.2022.101641

Ussher, J. R., and Drucker, D. J. (2023). Glucagon-like peptide 1 receptor agonists: cardiovascular benefits and mechanisms of action. *Nat. Rev. Cardiol.* 20 (7), 463–474. doi:10.1038/s41569-023-00849-3

Wang, J., Irnaten, M., Neff, R. A., Venkatesan, P., Evans, C., Loewy, A. D., et al. (2001). Synaptic and neurotransmitter activation of cardiac vagal neurons in the nucleus ambiguus. *Ann. N. Y. Acad. Sci.* 940, 237–246. doi:10.1111/j.1749-6632.2001.tb03680.x

Wei, Y., and Mojsov, S. (1995). Tissue-specific expression of the human receptor for glucagon-like peptide-I: brain, heart and pancreatic forms have the same deduced amino acid sequences. *FEBS Lett.* 358 (3), 219–224. doi:10.1016/0014-5793(94)01430-9

Wei, Y., and Mojsov, S. (1996). Distribution of GLP-1 and PACAP receptors in human tissues. *Acta Physiol. Scand.* 157 (3), 355–357. doi:10.1046/j.1365-201X.1996. 42256000.x

Woo, J. S., Kim, W., Ha, S. J., Kim, J. B., Kim, S. J., Kim, W. S., et al. (2013). Cardioprotective effects of exenatide in patients with ST-segment-elevation myocardial infarction undergoing primary percutaneous coronary intervention: results of exenatide myocardial protection in revascularization study. *Arterioscler. Thromb. Vasc. Biol.* 33 (9), 2252–2260. doi:10.1161/ATVBAHA.113.301586

Yang, Y., He, L., Liu, P., Wang, J., Yang, N., Li, Z., et al. (2024). Impact of a dual glucose-dependent insulinotropic peptide/glucagon-like peptide-1 receptor agonist tirzepatide on heart rate among patients with type 2 diabetes: a systematic review and pairwise and network meta-analysis. *Diabetes Obes. Metab.* 26 (2), 548–556. doi:10. 1111/dom.15342

Yaniv, Y., Ganesan, A., Yang, D., Ziman, B. D., Lyashkov, A. E., Levchenko, A., et al. (2015). Real-time relationship between PKA biochemical signal network dynamics and increased action potential firing rate in heart pacemaker cells: kinetics of PKA activation in heart pacemaker cells. *J. Mol. Cell Cardiol.* 86, 168–178. doi:10.1016/j.yjmcc.2015.07.024

Younce, C. W., Burmeister, M. A., and Ayala, J. E. (2013). Exendin-4 attenuates high glucose-induced cardiomyocyte apoptosis *via* inhibition of endoplasmic reticulum stress and activation of SERCA2a. *Am. J. Physiol. Cell Physiol.* 304 (6), C508–C518. doi:10.1152/ajpcell.00248.2012